ANNALS OF GEOPHYSICS, 67, 4, S432, 2024; doi:10.4401/ag-9162
OPEN ACCESS

An Unambiguous Signature of Pore Fluid Aftershock Triggering in the Landers Earthquake Sequence

Gregory C. Beroza[*,1], Eva E. Zanzerkia[2]

(1) Department of Geophysics, Stanford University, Stanford, CA, USA
(2) National Science Foundation, Alexandria, VA, USA

Article history: received September 20, 2024; accepted October 05, 2024

Abstract

Aftershocks within an extensional fault discontinuity of the 1992 Landers, California earthquake rupture occurred at an approximately constant rate for over three years following the mainshock. This contrasts with most of the rest of the aftershock sequence, and aftershock sequences in general, for which aftershock rates decay following Omori's law. The protracted aftershocks in the fault discontinuity can be understood if pore fluids are present at seismogenic depths and trigger seismicity as they flow to equilibrate pore pressure during the transition from the immediate, undrained to the eventual, drained condition. Changes in pore fluid pressure modulated by changes in the mean normal stress provide a clear and unambiguous signature of fluid effects in earthquake triggering. If this result generalizes to other settings, it suggests a predictable time-dependent component to the pattern of aftershock triggering not accounted for in models of Coulomb static stress triggering.

Keywords: Earthquakes; Aftershocks; Forecasting; Fluids; Stress

1. Introduction

The lack of a heat flow anomaly (Brune et al., 1969; Lachenbruch and Sass, 1980), the state of near fault-normal maximum compressive stress (Zoback et al., 1987) near major fault zones, as well as other stress indicators (Beroza and Zoback, 1992; Chester and Chester, 1998; Fialko et al., 2005; Fulton et al., 2013), suggest that fault slip during earthquakes occurs at much lower stress levels than predicted by laboratory friction. The notion that high pore fluid pressure allows faults to slip at lower shear stress by reducing the effective normal stress was introduced to explain overthrust faulting by Hubbert and Rubey (1959). There is ample geologic evidence that fluids and faults interact (Hickman et al., 1985; Sibson, 1994) and ample geophysical evidence that high fluid pressures occur in fault zones (Unsworth et al., 1997; Thurber et al., 1997).

Fluid injection has been shown to trigger earthquakes (Healy et al., 1968) and changes in fluid injection have been used to manipulate earthquake rates in the Rangeley earthquake control experiment (Raleigh et al., 1976). The role of fluids in triggering induced earthquakes is overwhelming and has been highlighted by the occurrence of widespread seismicity associated with unconventional hydrocarbon development in the Central United States and elsewhere (Schultz et al., 2020). Fluid triggering with pore fluid migration has also been used to explain earthquake swarms (Hainzl, 2004; Ross et al., 2020), but evidence that fluids play an important role in triggering tectonic earthquakes remains circumstantial.

In this paper we present evidence for pore-fluid earthquake triggering in the 1992 Landers, aftershock sequence. The effect can be clearly observed due to the large and predictable change in mean normal stress caused by strike-slip faulting on both sides of the fault discontinuity between the Johnson Valley and Homestead Valley faults. Pore fluid pressure migration in response to mainshock-induced pore pressure changes can explain the protracted aftershock sequence in the fault discontinuity, and this signature is difficult to ascribe to other processes. Such discontinuities are already known to be areas where fluid flow may be enhanced through repeated faulting (Sibson, 1986) so it is unclear to what extent this mechanism of earthquake triggering generalizes. Should it generalize, however, it would introduce a predictive time-dependence to Coulomb stress triggering that is not accounted for in current models of aftershock forecasting (Hardebeck et al., 2024).

2. Landers Aftershocks and Omori's Law

The 1992 Landers, California earthquake ruptured three major faults: the Johnson Valley, Homestead Valley, and Camp Rock-Emerson Faults, from southeast to northwest with right-lateral strike-slip of up to ~6 m of surface slip over a total length of more than 85 km (Hauksson et al., 1993; Sieh et al., 1993). The earthquake ruptured through two prominent fault discontinuities: a large extensional fault offset between the Johnson Valley and Homestead Valley Faults, and a smaller extensional offset between the Homestead Valley and Camp-Rock Emerson Faults. Based on strong motion modeling (Cohee and Beroza, 1994), the amount of slip at depth varied, but largely reflected the slip observed at the Earth's surface.

We base our analysis of the Landers aftershocks on the standard catalog of the Southern California Earthquake Data Center (SCEDC, 2013). In aggregate, the extensive aftershock sequence following the mainshock followed the well-known and long-established Omori's law (Omori, 1894) as modified by Utsu (1961), which holds that the rate of aftershocks R, decays with time, t, following a large earthquake as $R(t) \sim (t + c)^{-p}$, where c is a constant and the exponent, p, is ~1. Aftershocks are thought to occur in response to the stress change imposed by the mainshock they follow (Scholz, 1990), but the source of the delay in their occurrence is less clear. Elastic effects act immediately, and do not explain the gradual decay with time, but multiple mechanisms have been suggested to explain the delay described by Omori's law, including: stress corrosion (Scholz, 1968), earthquake nucleation under rate- and state-variable friction (Dieterich, 1994), viscoelastic relaxation (Freed and Lin, 2001), afterslip under rate-strengthening friction on the deep extension of the fault (Perfettini and Avoac, 2007) and interactions in a spring-block-slider model (Petrillo et al., 2020). Another proposed mechanism for the delay invokes processes associated with pore fluid flow (Nur and Booker, 1972).

In a fluid-infiltrated, porous elastic medium, a pore pressure decrease will occur where the mean normal stress decreases and a pore pressure increase will occur where the mean normal stress increases (Rice and Cleary, 1976). The change in pore pressure, P for undrained conditions can be related to the change in the mean normal stress, s_{kk}, as: $DP = B\sigma_{kk}$, where Skempton's coefficient, B, a function of elastic moduli for drained and undrained conditions, is equal to one for fluid saturated soils and ranges between 0.5 and 0.9 for a range of rock types increases (Rice and Cleary, 1976). With time, this undrained state evolves to the drained state as fluids flow and re-equilibrate in response to the induced pore pressure gradients. This adjustment can trigger earthquakes by inducing shear stress through poro-elastic consolidation of regions that underwent changes in mean normal stress in the mainshock. In the undrained state, changes in the mean normal stress will be effectively buffered by changes in pore pressure. This effect will diminish during the transition to drained conditions and induce changes in shear stress that can trigger aftershocks (Booker, 1974).

Fluids can also trigger aftershocks through changes in the effective normal stress (Terzhagi, 1943) that occur due to the transition from undrained to drained conditions. Under the Coulomb failure criterion (Harris, 1998), faulting will occur when the shear stress, τ, exceeds the sum of the cohesion, C, and the effective normal stress multiplied by the coefficient of friction, μ:

$$\tau > \mu\,(\sigma - P) + C \tag{1}$$

where the effective normal stress is the difference of the normal stress, σ, and the pore pressure, P, and the cohesion is thought to be small for faults in the Earth (Sibson, 1986). In the presence of pore fluids, P, will be time dependent and if the pore pressure increases with time an earthquake may be triggered without changes in the shear stress.

3. Landers Aftershocks and Pore-Fluid Triggering

A distinguishing characteristic of poro-elastic models is the role of the mean normal stress (Nur and Booker, 1972). Fault-zone discontinuities, where changes in mean normal stress are both large and predictable (Segall and Pollard, 1980), present an opportunity to search for pore-fluid earthquake triggering. Faults are complex at all scales (Tchalenko, 1970), with some discontinuities large enough to be expressed in the mapped surface trace. Large fault discontinuities are not just surficial, but extend through seismogenic depths (Felzer and Beroza, 1999), and they are thought to influence earthquake size (Schwartz and Coppersmith, 1984; Philibosian and Meltzner, 2020). Fault offsets are classified as *compressional* if faulting leads to compression (mean normal stress increase) between the two fault segments or *extensional* if faulting leads to extension (mean normal stress decrease). As we argue below, for an extensional discontinuity, pore fluid effects predict a protracted aftershock sequence (Fig. 1) and for a compressional discontinuity, pore fluid effects predict an abbreviated aftershock sequence relative to what would otherwise occur.

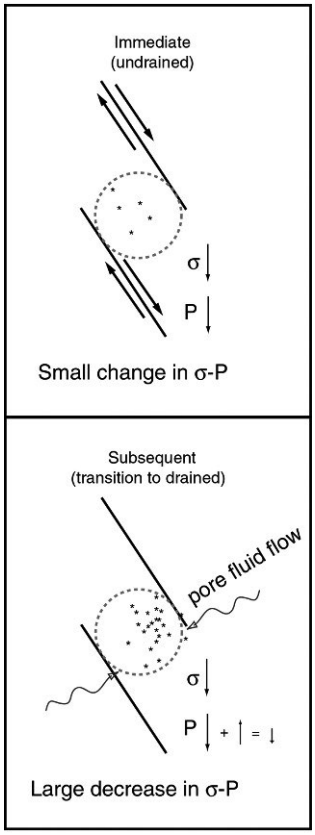

Figure 1. Schematic explanation of protracted aftershocks in an extensional discontinuity. Stars represent aftershocks and dashed circle represents area within the discontinuity where mean normal stress decreases. Faulting on both sides of the discontinuity leads to a mean normal stress decrease within it. Immediately after the mainshock, many aftershocks will be inhibited because the drop in normal stress will be offset by a pore pressure decrease. As pore pressure gradients induce pore fluids to migrate (wavy lines) into the discontinuity, the pore pressure will increase, the effective normal stress will decrease, and aftershocks will be triggered. In a compressional discontinuity, the sense of the changes is reversed such that the mean normal stress increases and pore fluid flow will tend to lock potential aftershock fault planes resulting in an abbreviated aftershock sequence.

Within an extensional discontinuity the mean normal stress will decrease and hence the normal stress, σ, acting across potential fault planes within the discontinuity will also tend to decrease, but the pore pressure will decrease as well. Thus, if fluids are present, the right-hand side of (1) will not change as much as if pore fluids were absent and relatively few aftershocks will be triggered immediately after the mainshock. This is the undrained response.

Over time, as pore fluids flow in response to the induced pore pressure gradients, the pore pressure decrease will decay, but the normal stress change will not. Thus, as the medium drains, the effective normal stress, $\sigma - P$, will decrease and tend to unlock potential aftershock fault planes. This will trigger late aftershocks resulting in a protracted aftershock sequence. For a compressional discontinuity, the sign of the mean normal stress and pore pressure changes are reversed, the sense of fluid flow would be reversed, the effective normal stress will tend to increase with time, and the result will be an abbreviated aftershock sequence.

In Fig. 2 we divide the aftershock zone into subareas that extend 5 km to either side of the fault trace. Within each of these subareas we plot the cumulative number of aftershocks against time after the mainshock.

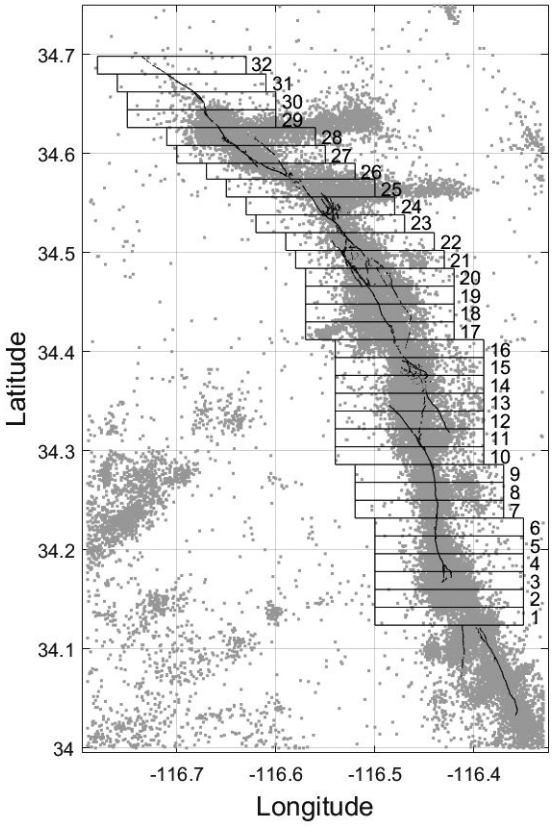

Figure 2. Map showing Landers surface rupture in black, aftershocks in gray, together with boxes used to examine temporal dependence of aftershock seismicity.

The curves in Fig. 3 show that for most of the fault the aftershocks accumulate rapidly shortly following the mainshock, with the rate gradually decreasing, as Omori's law predicts. Areas 11-16 behave in a similar fashion to the other areas for the first 6 months after the mainshock; however, thereafter they show a distinctly different behaviour. For about 3 years, each of these areas shows an approximately constant aftershock rate.

As with all aftershock catalogs, the magnitude of completeness is high in the period of intense activity following the mainshock, before returning to normal when the frequency of aftershocks subsides (Lippiello et al., 2019). Because we compare relative aftershock rates for different parts of the aftershock sequence, the time-dependence in the magnitude of completeness will not affect our results. Spatial variations in the magnitude of completeness are also known to occur. These protracted aftershocks are not attributable to variations in the network detection threshold because the detectability threshold for the Landers aftershock sequence changes only gradually from south to north due to variations in seismic network coverage. A rate change resulting from changes in network coverage would act over much larger spatial scales than the variations we observe (Schorlemmer and Woessner, 2008) and would include adjacent straight segments of the fault where the aftershock decay is normal. The protracted aftershock signature spans several contiguous bins, is robust with respect to the dimensions of the area considered

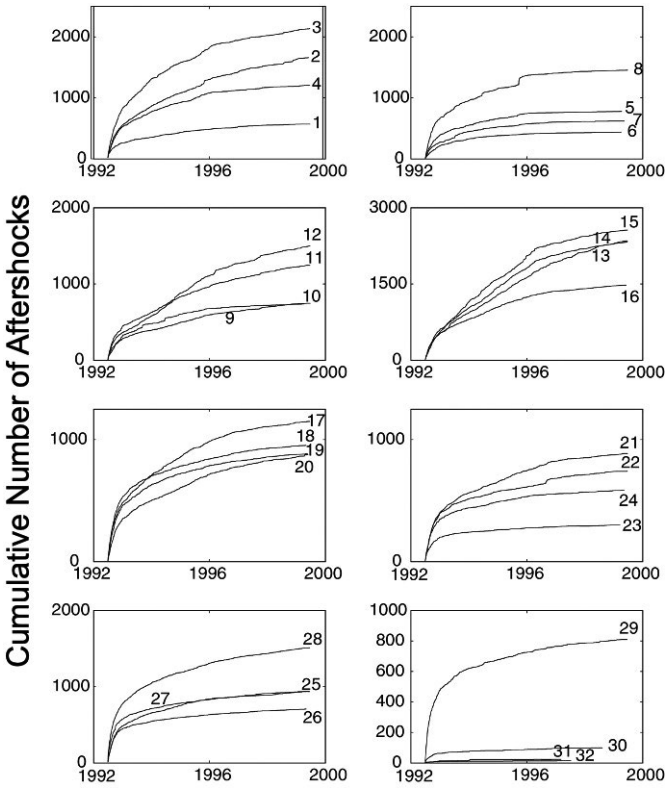

Figure 3. Cumulative number of aftershocks with time for the boxes in Fig. 2. The protracted aftershocks appear most clearly as a trend of approximately constant slope for boxes 11-16 from 0.5 to 3.5 years after the Landers mainshock. This straight line behaviour represents a constant aftershock rate rather than the decay predicted by Omori's law.

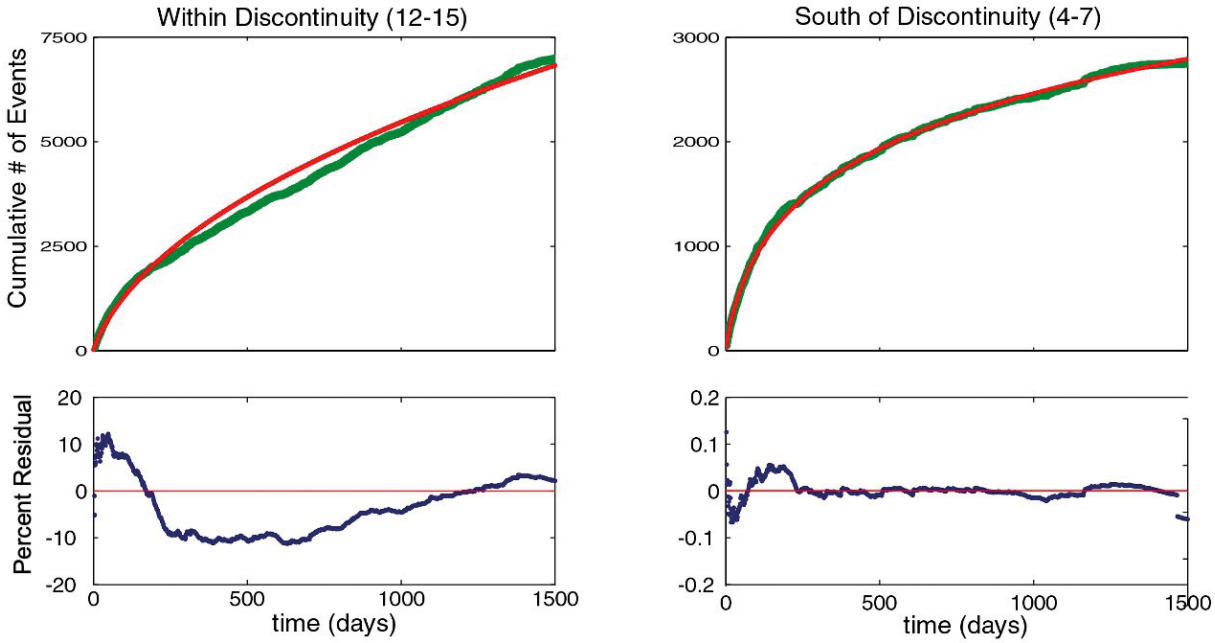

Figure 4. Fit (red) of the accumulation of aftershocks (green) to the modified Omori's law for aftershocks clearly within (left panels) and outside of (right panels) the large fault discontinuity. Best fit to aftershocks within the discontinuity has an exceptionally low p value of 0.55 (slow decay rate); moreover, a x^2 test indicates the data residuals (lower panel) are inconsistent with the modified Omori's law at the 95% confidence level. For aftershocks outside of the discontinuity we find a normal p value of 0.9 and a x^2 test indicates that this model provides an adequate fit to the data.

and is not attributable to secondary aftershock sequences following one or several large aftershocks. The protracted aftershocks are situated directly within the most prominent extensional offset in the fault trace and suggest that pore fluid effects play an important role in aftershock triggering.

We note that these aftershocks represent a statistically significant failure of Omori's law to describe the data, not simply a relatively low decay that manifests as a low p value as observed in some instances (Schaff et al., 1988; Wiemer and Katsumata, 1999). Figure 4 shows the residuals vs. time after a fit of the accumulation of aftershocks to the modified Omori's law for aftershocks.

The best fit within the discontinuity has an exceptionally low p value of 0.55. That is, it shows a very slow decay; however, even with that slow decay, the fit is not very good, with a large and systematic misfit in the residuals. A X^2

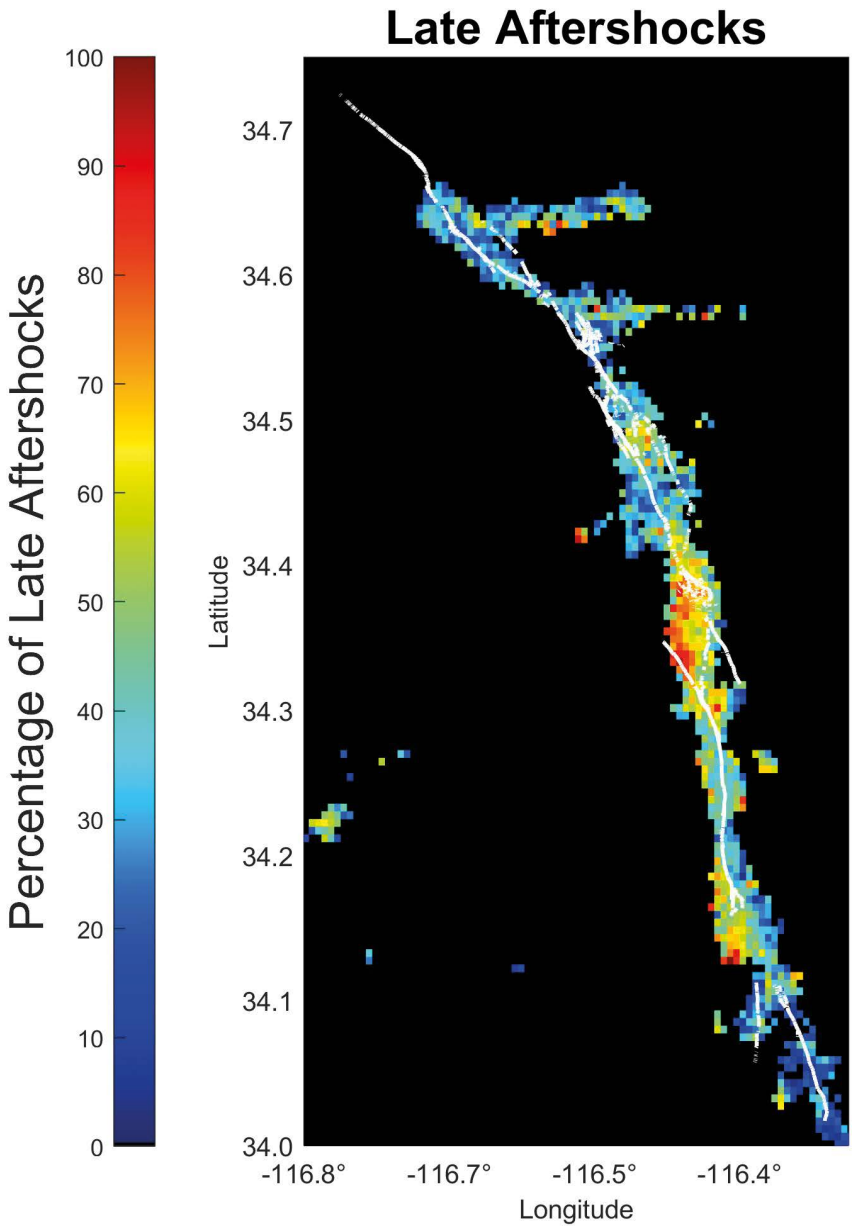

Figure 5. Relative aftershock rate displayed as the percentage of aftershocks in years 1 and 3 following the mainshock that occurred in year 3. Instances of less that 8 total aftershocks within each 0.01 by 0.01 degree box are not plotted. Areas of protracted aftershocks (relatively more aftershocks at later times) show as warm colours (green to red). These are most prominent in the large extensional discontinuity between the Johnson Valley (JV) and Homestead Valley (HV) faults and at the southern end of the rupture. The extensional discontinuity between the Homestead Valley and Camp Rock/Emerson (CR) faults also shows a protracted aftershock sequence, though the effect is subtle. Straight segments of faults plot as cool colours, consistent with decay of the aftershock rate with time.

test indicates that the level of misfit is inconsistent with the modified Omori's law at the 95% confidence level. For aftershocks outside of the discontinuity can be fit with a normal p value of 0.9 and a x^2 test indicates an adequate fit to the data (Fig. 4).

We can get a clearer view of the spatial extent of protracted aftershocks by considering smaller areas and using a simple measure of aftershock decay. Figure 5 shows how closely the protracted aftershocks are confined within the discontinuity between the Johnson Valley and Homestead Valley faults.

The short scale length of the effect precludes viscoelasticity of the lower crust, which would operate over much larger spatial scales. Freed and Lin (2001) show that the spatial scales of the viscoelastic response are comparable to, or longer than, the thickness of the elastic crust. Nucleation under a rate- and state-variable friction law does not explain our observations either as it predicts no difference in time dependence outside vs. inside the discontinuity.

There are several other small, localized areas in Fig. 5 that show a protracted aftershock sequence. Near the southern end of the surface rupture there is another prominent area of protracted aftershocks. The surface rupture bifurcates and terminates in this region, so it is difficult to assess whether this activity might also be attributed to the same pore-fluid effects. We also observe protracted aftershock activity in the smaller offset between the Homestead Valley and Camp Rock-Emerson faults (Fig. 5), but the effect is more subtle. There is a small compressional offset along the Camp Rock-Emerson fault, but evidence for an abbreviated aftershock sequence at this location is equivocal. It is interesting that aftershocks on the straight fault segments consistently show a rapid decay. This indicates that the mechanism proposed by Booker (1974), in which the poroelastic response leads to shear loading that triggers aftershocks, does not appear to be operative.

We note that fluid effects have been independently inferred from post-seismic InSAR measurements for this earthquake (Peltzer et al., 1996) and the effect was seen most prominently in the same Johnson Valley-Homestead Valley fault offset that is highlighted in this study. The surface deformation was centered on the fault trace; however, while the protracted aftershocks were located to the west of the fault trace. The difference may be attributable to changes in the fault geometry and slip distribution with depth. The decay time for poro-elastic effects in the surface deformation was 270 days (Peltzer et al., 1998), rather than ~3 years as we have found, and the depth of the source of the deformation anomaly was modeled as 0-4 km. The protracted seismicity extends to depths of 8 km, and the longer duration of the effect in the aftershocks is consistent with an expected decrease in hydraulic diffusivity with increasing depth (Ingebritson and Manning, 2010).

It is ironic that the signature of pore-fluid triggering is manifest as a violation of Omori's law, given that Omori's law was the property of aftershock sequences that pore fluid effects were originally invoked to explain; however, we note that the theory was developed for aftershock decay on a planar fault and that the three-dimensional structure of fault discontinuities and the complex and variable permeability structure of fault zones and their surroundings may confound specific predictions.

4. Conclusions

The protracted aftershocks in the Landers aftershock sequence suggest that fluids at seismogenic depths play an important role in the earthquake process, and specifically in earthquake triggering. Others have suggested that pore fluids may have triggered aftershocks of the Landers earthquake (Bosl and Nur, 2002; Miller, 2020) and the Landers sequence is not the only one in which pore fluid triggering has been hypothesized (Li et al., 1987; Hudnut and Seeber, 1989). What distinguishes our results is the particularly clear and unambiguous signature of pore fluids due to the large and predictable change in mean normal stress in the fault discontinuity, that the temporal dependence of fluid flow leads to a time-dependent response, and that the temporal and spatial distribution of the signal are not readily explained by other mechanisms.

It remains unclear how important pore fluid effects are for earthquake triggering more generally for other earthquake sequences and other tectonic settings. The mean normal stress is nodal along the fault plane for a uniform planar fault, which will make it difficult to evaluate its possible role in triggering most aftershocks; however, there are other situations in which the signature of pore fluids may be recognizable. For example, earthquakes that have prominent off-fault aftershock sequences ought to show an asymmetry in their temporal decay that becomes more prominent with time. Evidence for such behaviour has not been widely reported, but it appears to occur at least in some cases (Li et al., 1987).

Data availability statement. Data can be downloaded at: https://scedc.caltech.edu/data/eq-catalogs.html.

Acknowledgements. We thank J. Dieterich, M. Guatteri, L. Jones, S. Miller, A. Nur, S. Rojstaczer, P. Segall, K. Felzer, and R. Sibson, for their helpful comments. The views represented are not necessarily those of the U.S. Federal government or of the U.S. National Science Foundation. This work supported by USGS grant 00HQGR0062.

References

Beroza, G. C. and M. D. Zoback (1993). Mechanism diversity of the Loma Prieta aftershocks and the mechanics of mainshock-aftershock interaction, Science, 259, 5092, 210-213, doi:10.1126/science.259.5092.21.

Booker, J. R. (1974). Time dependent strain following faulting of porous medium, J. Geophys. Res., 79, 2037-2044, doi:10.1029/JB079i014p02037.

Bosl, W. J. and A. Nur (2002). Aftershocks and pore fluid diffusion following the 1992 Landers earthquake, J. Geophys. Res., 107, B12, 2366, doi:10.1029/2001JB000155.

Brune, J. N., T. L. Henyey and R. F. Roy (1967). Heat flow, stress, and rate of slip along the San Andreas fault, California, J. Geophys. Res., 74, 3821-3827, doi:10.1029/JB074i015p03821.

Lippiello, E., A. Cirillo, C. Godano, E. Papadimitriou et al. (2019). Post seismic catalog incompleteness and aftershock forecasting, Geosciences, 9, 8, 355, doi:10.3390/geosciences9080355.

Chester, F. M. and J. S. Chester (1998). Ultracataclasite structure and friction processes of the Punchbowl fault, San Andreas system, California, Tectonophysics, 295, 1-2, 199-221, doi:10.1016/S0040-1951(98)00121-8.

Cohee, B. P. and G. C. Beroza (1994). Slip distribution of the 1992 Landers earthquake and its implications for earthquake source mechanics, Bull. Seismol. Soc. Am., 84, 3, 692-712, doi:10.1785/BSSA0840030692.

Dieterich, J. H. (1994). A constitutive law for rate of earthquake production and its application to earthquake clustering, J. Geophys. Res., 99, 2601-2618, doi:10.1029/93JB02581.

Felzer, K. R. and G. C. Beroza (1999). Deep structure of a fault discontinuity, Geophys. Res. Lett., 26, 2121-2124, doi:10.1029/1999GL900484.

Fialko, Y., L. Rivera and H. Kanamori (2005). Estimate of differential stress in the upper crust from variations in topography and strike along the San Andreas fault, Geophys. J. Int., 160, 2, 527-532, doi:10.1111/j.1365-246X.2004.02511.x.

Freed, A. M. and J. Lin (2001). Delayed triggering of the 1999 Hector Mine earthquake by viscoelastic stress transfer, Nature, 411, 180-183, 10.1038/35075548.

Fulton, P. M., E. E. Brodsky, Y. Kano, J. Mori et al. (2013). Low coseismic friction on the Tohoku-Oki fault determined from temperature measurements, Science, 342, 6163, 1214-1217, 10.1126/science.1243641.

Hainzl, S. (2004). Seismicity patterns of earthquake swarms due to fluid intrusion and stress triggering, Geophys. J. Int., 159, 3, 1090-1096, doi:10.1111/j.1365-246X.2004.02463.x.

Hardebeck, J. L., A. L. Llenos, A. J. Michael, M. T. Page et al. (2024). Aftershock Forecastin, Ann. Rev. Earth Planet Sci., 52, doi:10.1146/annurev-earth-040522-102129.

Harris, R. A. (1998). Introduction to special section: Stress triggers, stress shadows, and implications for seismic hazard, J. Geophys. Res., 103, 24,347-24,358, 10.1029/98JB01576.

Hauksson, E., L. M. Jones, K. Hutton and D. Eberhart-Phillips (1993). The 1992 Landers earthquake sequence: seismological observations, J. Geophys. Res., 98, 19835-19858, 10.1029/93JB02384.

Healy, J. H., W. W. Rubey, D. T. Griggs and C. B. Raleigh (1968). The Denver Earthquakes, Science, 161, 1301-1310, 10.1126/science.161.3848.130.

Hickman, S., R. Sibson and R. Bruhn (1985). Introduction to Special Section: Mechanical Involvement of Fluids in Faulting, J. Geophys. Res., 100, 12,831-12,840, 10.1029/95JB01121.

Hubbert, M. K. and W. W. Rubey (1959). Role of fluid pressure in mechanics of overthrust faulting: I. mechanics of fluid-filled porous solids and its application to overthrust faulting, Geol. Soc. Am. Bull., 70, 2, 115-166, doi:10.1130/0016-7606(1959)70.

Hudnut, K. W., L. Seeber and J. Pacheco (1989). Cross-fault triggering in the November 1987 Superstition Hills earthquake sequence, southern California, Geophys. Res. Lett. 16, 199-202, doi:10.1029/GL016i002p00199.

Ingebritsen, S. E. and C. E. Manning (2010). Permeability of the continental crust: dynamic variations inferred from seismicity and metamorphism, Geofluids, 10, 1-2, 193-205, doi:10.1111/j.1468-8123.2010.00278.x.

Lachenbruch, A. H and J. H. Sass (1980). Heat flow and energetics of the San Andreas fault zone, J. Geophys. Res., Solid Earth, 85, B11, 6185-6222, doi:10.1029/JB085iB11p06185.

Li, V. C., S. H. Seale and T. Cao (1987). Postseismic stress and pore pressure readjustment and aftershock distributions, Tectonophysics, 144, 37-54, 10.1016/0040-1951(87)90007-2.

Miller, S. A. (2020). Aftershocks are fluid-driven and decay rates controlled by permeability dynamics, Nat. Commun., 11, 1, 5787, doi:10.1038/s41467-020-19590-3.

Nur, A. and J. R. Booker (1972). Aftershocks caused by pore fluid flow? Science, 175, 885-887, 10.1126/science.175.4024.885.

Omori, F. (1894). On after-shocks of earthquakes, J. Coll. Sci. Imp. Univ. Tokyo, 7, 111-200.

Peltzer, G., P. Rosen, F. Rogez and K. Hudnut (1996). Postseismic rebound in fault step-overs caused by pore fluid flow, Science, 273, 1202-1204, 10.1126/science.273.5279.1202.

Peltzer, G., P. Rosen, F. Rogez, and K. Hudnut (1998). Poroelastic rebound along the Landers 1992 earthquake surface rupture, J. Geophys. Res., 103, 30, 13130, 145, doi:10.1029/98JB02302.

Perfettini, H. and J. P. Avouac (2007), Modeling afterslip and aftershocks following the 1992 Landers earthquake, J. Geophys. Res., 112, B07409, doi:10.1029/2006JB004399.

Petrillo, G., E. Lippiello, F. P. Landes and A. Rosso (2020). The influence of the brittle-ductile transition zone on aftershock and foreshock occurrence, Nat. Commun., 11, 1, 3010, doi:10.1038/s41467-020-16811-7.

Philibosian, B. and A. J. Meltzner (2020). Segmentation and supercycles: A catalog of earthquake rupture patterns from the Sumatran Sunda Megathrust and other well-studied faults worldwide, Quat. Sci. Rev., 241, 106390, doi:10.1016/j.quascirev.2020.106390.

Raleigh, C. B., J. H. Healy and J. D. Bredehoeft (1976). An Experiment in Earthquake Control at Rangely, Colorado, Science, 191, 1230-1237, 10.1126/science.191.4233.1230.

Rice J. R. and M. P. Cleary (1976). Some basic stress diffusion solutions for fluid-saturated elastic porous media with compressible constituents, Rev. Geophys. Space Phys., 14, 227-241, doi:10.1029/RG014i002p00227.

Ross, Z. E., E. S. Cochran, D. T. Trugman and J. D. Smith (2020). 3D fault architecture controls the dynamism of earthquake swarms, Science, 368, 6497, 1357-1361, 10.1126/science.abb0779.

Schaff, D. P., G. C. Beroza and B. E. Shaw (1988). Postseismic response of repeating aftershocks, Geophys. Res. Lett., 24, 4549-4552, doi:10.1029/1998GL900192.

Scholz, C. H. (1968). Microfractures, aftershocks, and seismicity, Bull. Seismol. Soc. Am., 58, 1117-1130, doi:10.1785/BSSA0580031117.

Scholz, C. H. (1990). The Mechanics of Earthquakes and Faulting, Cambridge University Press, New York, doi:10.1017/CBO9780511818516.

Schorlemmer, D. and J. Woessner (2008). Probability of detecting an earthquake, Bull. Seismol. Soc. Am., 98, 5, 2103-2117, 10.1785/0120070105.

Schultz, R., R. J. Skoumal, M. R. Brudzinski, D. Eaton et al. (2020). Hydraulic fracturing-induced seismicity, Rev. Geophys., 58, 3, e2019RG000695, doi:10.1029/2019RG000695.

Schwartz, D. P. and K. J. Coppersmith (1984). Fault behavior and characteristic earthquakes: Examples from the Wasatch and San Andreas fault zones, J. Geophys. Res., 89, B7, 5681-5698, doi:10.1029/JB089iB07p05681.

SCEDC (2013). Southern California Earthquake Center, Caltech, Dataset, doi:10.7909/C3WD3xH.

Segall, P. and D. M. Pollard (1980). Mechanics of discontinuous faults, J. Geophys. Res., 85, 4337-4350, doi:10.1029/JB085iB08p04337.

Sibson, R. H. (1986). Rupture interaction with fault jogs, Earthquake source mechanics, 37, 157-167, 10.1029/GM037p0157.

Sibson, R. H. (1994). Crustal stress, faulting and fluid flow, Geol. Soc., London, Special Publications, 78, 1, 69-84, 10.1144/GSL.SP.1994.078.01.07.

Sieh, K., L. Jones, E. Hauksson, K. Hudnut et al. (1993). Near-field investigations of the Landers earthquake sequence, April to July 1992, Science, 260, 171-176, 10.1126/science.260.5105.171.

Tchalenko, J. S. (1970). Similarities between shear zones of different magnitudes, Bull. Geol. Soc. Am., 81, 1625-1640, 10.1130/0016-7606(1970)81[1625:SBSZOD]2.0.CO;2.

Terzaghi, K. (1943). Theoretical soil mechanics, John Wiley and Sons, Inc., New York, 10.1002/9780470172766.

Thurber, C., S. R. Roecker, W. L. Ellsworth, Y. Chen et al. (1997). Two-dimensional seismic image of the San Andreas fault in the Northern Gabilan Range, central California: Evidence for fluids in the fault zone, Geophys. Res. Lett., 24,1591-1594, 10.1029/97GL01435.

Unsworth, M. J., P. E. Malin, G. D. Egbert and J. R. Booker (1997). Internal Structure of the San Andreas fault at Parkfield, California, Geology, 25, 359-362, doi:10.1130/0091-7613(1997)025<0359:ISOTSA>2.3.CO;2.

Utsu, T. (1961). A statistical study on the occurrence of aftershocks, Geophys. Mag., 30, 521-605.

Wiemer, S. and K. Katsumata (1999). Spatial variability of seismicity parameters in aftershock zones, J. Geophys. Res., 104, 13,135-13,151, doi:10.1029/1999JB900032.

Zoback, M. D., M. L. Zoback, V. S. Mount, J. Suppe et al. (1987). New evidence on the state of stress of the San Andreas fault system, Science, 238, 4830, 1105-1111, 10.1126/science.238.4830.1105.

***CORRESPONDING AUTHOR: Gregory BEROZA**,
Department of Geophysics, 397 Panama Mall, Stanford, CA, 94305-2215, USA
e-mail: beroza@stanford.edu